Disorder Scattering in Magnetic Tunnel Junctions: Theory of Nonequilibrium Vertex Correction

Youqi Ke,[1] Ke Xia,[2] and Hong Guo[1]

[1]*Centre for the Physics of Materials and Department of Physics, McGill University, Montreal, PQ, H3A 2T8, Canada*
[2]*State Key Laboratory for Surface Physics, Institute of Physics, Chinese Academy of Sciences, P.O. Box 603, Beijing 100080, China*

(Received 16 December 2007; published 25 April 2008)

We report a first principles formalism and its numerical implementation for treating quantum transport properties of nanoelectronic devices with atomistic disorder. We develop a nonequilibrium vertex correction (NVC) theory to handle the configurational average of random disorder at the density matrix level so that disorder effects to nonlinear and nonequilibrium quantum transport can be calculated from atomic first principles in a self-consistent and efficient manner. We implement the NVC into a Keldysh nonequilibrium Green's function (NEGF) -based density functional theory (DFT) and apply the NEGF-DFT-NVC formalism to Fe/vacuum/Fe magnetic tunnel junctions with interface roughness disorder. Our results show that disorder has dramatic effects on the nonlinear spin injection and tunnel magnetoresistance ratio.

DOI: 10.1103/PhysRevLett.100.166805 PACS numbers: 85.35.−p, 72.25.Mk, 73.63.Rt, 75.47.De

Quantitative understanding of impurity effects is crucial for nanoelectronics where device properties are strongly influenced by or even built on such effects. Examples are electron scattering by dopants in semiconductor nanowires [1] and field effect transistors, spin scattering by disorder in magnetic tunnel junctions [2], and transport of spin-polarized current in dilute magnetic semiconductors [3]. Unintentional impurities sit inside a device at unpredictable locations, and, therefore, any physical quantity predicted by theory should be averaged over impurity configurations. In *ab initio* calculations, one may carry out this average by generating many impurity configurations for a given concentration x, calculating the relevant physical quantity for each configuration, and finally averaging the results. Such a brute force calculation is often not practical for at least two reasons. First, when x is small as is typical in the case of semiconductor devices, say, 0.1%, one would need a thousand host atoms to accommodate just one impurity atom. Second, it is known that an impurity average may require a huge number of configurations [4]. These requirements make a calculation prohibitively large. Considerable effort has therefore been devoted in the literature to develop approximate techniques which avoid brute force. In this regard, a widely used technique is the coherent potential approximation (CPA) [5] as implemented in the Korringa-Kohn-Rostoker [6] and linear muffin-tin orbital (LMTO) [7] first principles methods. So far, CPA has been applied to *equilibrium* electronic structure and transport calculations [8]. However, most nanoelectronic devices operate under *nonequilibrium* conditions; for instance, one wishes to predict nonlinear current-voltage (I-V) characteristics. It is thus very important to develop appropriate nonequilibrium techniques for impurity averaging.

Here we report our solution of the atomistic nonequilibrium impurity average problem for quantum transport. We start from a state-of-the-art real space atomistic quantum transport formalism where density functional theory (DFT) is carried out within the Keldysh nonequilibrium Green's function (NEGF) framework [9,10]. The basic idea of NEGF-DFT is that the device Hamiltonian and the electronic structure are determined by DFT, the nonequilibrium quantum statistics of the device physics is determined by NEGF, and the transport boundary conditions under external bias are handled by a real space numerical technique. We deal with an impurity average at the single particle retarded Green's function level by CPA [5] and at the NEGF level by evaluating a nonequilibrium vertex correction (NVC) term. The NEGF-DFT-NVC formalism allows us to construct a nonequilibrium density matrix self-consistently that includes impurity averaging. We then apply our NEGF-DFT-NVC formalism to investigate the effects of interface roughness disorder in a magnetic tunnel junction (MTJ). Our results indicate that the disorder effect can drastically and qualitatively influence the nonlinear I-V curves and tunnel magnetoresistance ratio.

We consider a two-probe device consisting of a scattering region and two semi-infinite leads extending along the transport direction $\mathbf{z}$ to $z = \pm\infty$, as shown in Fig. 1. The system is periodically extended along the transverse (x, y) direction. Note that the scattering region includes several layers of lead atoms [9]. A bias voltage V_b is applied across

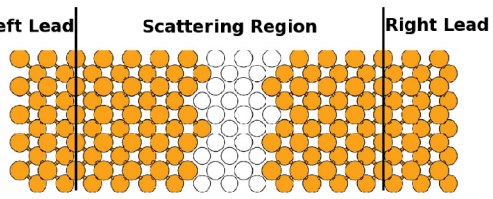

FIG. 1 (color online). Schematic of atomic structure of the Fe/Vac/Fe magnetic tunnel junction. The two Fe/Vac interfaces have roughness disorder. Fe: yellow spheres; vacuum: white spheres.

the leads to drive a current flow, i.e., $\mu_l - \mu_r = eV_b$, where $\mu_{l,r}$ are electrochemical potentials of the left or right leads. We assume that impurities exist inside the scattering region randomly but not in the leads. We further assume that any atomic position R in the scattering region may be occupied by two atomic species, the host and impurity atoms labeled by $Q = A, B$ with concentrations C_R^A and C_R^B such that $C_R^A + C_R^B = 1$.

In a NEGF-DFT self-consistent analysis [9] of *ordered* systems, the nonequilibrium density matrix is calculated by NEGF $\mathbf{G}^<(E)$, i.e., $\hat{n}(E) \sim \mathbf{G}^<(E)$; here, $G^<$ satisfies the Keldysh equation $G^< = G^{\mathcal{R}}\Sigma^< G^{\mathcal{A}}$, where $G^{\mathcal{R}} = (G^{\mathcal{A}})^\dagger$ is the retarded Green's function. $\Sigma^< = i\Gamma_l f_l + i\Gamma_r f_r$ is the lesser self-energy, where $f_{l,r}$ are Fermi functions of the left or right leads; $\Gamma_{l,r}$ are linewidth functions describing coupling of the scattering region to the leads, and they can be calculated by standard iterative methods [9]. Translational invariance of the ordered system allows one to evaluate all quantities in the unit cell by integration over the two-dimensional Brillouin zone (BZ) in the (x, y) direction. When there are impurities, translational symmetry is broken. The spirit of CPA is to construct an effective medium theory by an impurity configurational average that restores the translational invariance. For NEGF, this means calculating $\bar{G}^< = \overline{G^{\mathcal{R}}\Sigma^< G^{\mathcal{A}}}$. Even though there is no impurity in the leads to affect $\Sigma^<$, the impurity average $\overline{(\cdots)}$ correlates Green's functions $G^{\mathcal{R}}$ with $G^{\mathcal{A}}$. In particular, $\bar{G}^< \neq \bar{G}^{\mathcal{R}}\Sigma^<\bar{G}^{\mathcal{A}}$ due to multiple scattering by the impurities. To calculate $\bar{G}^<$, we introduce a quantity Ω_{NVC} that is a consequence of impurity scattering at nonequilibrium, such that $\bar{G}^< = \bar{G}^{\mathcal{R}}(\Sigma^< + \Omega_{\mathrm{NVC}})\bar{G}^{\mathcal{A}}$. Ω_{NVC} is called a NVC whose equilibrium counterpart is well known in calculations of the Kubo formula by Feynman diagrammatic techniques [11]. There is, however, a major qualitative difference here: Ω_{NVC} depends on the nonequilibrium quantum statistical information of the device scattering region, while the equilibrium VC does not.

We found that Ω_{NVC} is most conveniently calculable by using a *site-oriented* calculation scheme; for this reason, we develop our NEGF-NVC theory within the tight-binding (TB) LMTO DFT implementation [12,13], by using CPA [7,8] to describe the averaged system. In this approach, the impurity average for any single-site physical quantity X_R is given by

$$\bar{X}_R = \sum_{Q=A,B} C_R^Q \bar{X}_R^Q, \tag{1}$$

where $\bar{X}_R^Q$ is the conditional average over a particular atomic species Q at site R which is calculated by

$$\bar{X}_R^Q = \overline{\eta_R^Q X_R}/C_R^Q. \tag{2}$$

Here η_R^Q is the occupation of site R by atomic species Q, and its average is $\bar{\eta}_R^Q = C_R^Q$. Equation (1) means that the average of a quantity at site R is a linear combination of contributions from each atomic species.

The technical derivation details are given in the supplemental material associated with this Letter [14]; here, we briefly outline the spirit of the theory. The impurity average of the site diagonal NEGF is carried out by application of Eq. (1), i.e., $\bar{G}_{RR}^< = \sum_{Q=A,B} C_R^Q \bar{G}_{RR}^{<,Q}$. The atom-resolved NEGF $\bar{G}_{RR}^{<,Q}$ gives the atom-resolved average local charge density $\bar{n}_R^Q \sim \bar{G}_{RR}^{<,Q}$, which is needed in the DFT self-consistent iterations [9]. To find $\bar{G}_{RR}^{<,Q}$, we use Eq. (2). The final expressions of $\bar{G}_{RR}^{<,Q}$ are given in Eqs. (10), (28), and (29) of the supplemental material [14], and they are related to Ω_{NVC} of the auxiliary NEGF. The calculation of NVC is carried out by application of single-site approximation within CPA-based multiple scattering theory as summarized in the supplemental material [14], where the final expression is given by Eq. (23). From Ω_{NVC}, we obtain $\bar{G}_{RR}^{<,Q}$ and hence the averaged density matrix $\bar{n}_R^Q$ for atom Q on site R. The charge density is used to calculate the device Hamiltonian for the next step in the DFT iteration, and this procedure is repeated until numerical convergence.

An extremely stringent test of our NEGF-DFT-NVC formalism and its numerical implementation is carried out by calculating two-probe devices at equilibrium and checking if the fluctuation-dissipation relationship is satisfied or not. Mathematically, the fluctuation-dissipation theorem dictates that $\bar{G}_{RR}^{<,Q} = \bar{G}_{RR}^{\mathcal{A},Q} - \bar{G}_{RR}^{\mathcal{R},Q}$ at equilibrium. Here the calculation of $\bar{G}_{RR}^{<,Q}$ requires NVC, while calculations of $\bar{G}_{RR}^{\mathcal{A},Q}$ and $\bar{G}_{RR}^{\mathcal{R},Q}$ do not. For many disordered device structures, including that in Fig. 1, that we have checked, the fluctuation-dissipation relationship is always satisfied to at least one part in a million, and the final tiny difference can be attributed to numerical calculation issues. We found that NVC is extremely important: Without it, the density matrix and transmission coefficients can have large errors and even become qualitatively incorrect.

After the NEGF-DFT-NVC self-consistent calculation is converged, we calculate current-voltage (I-V) characteristics by the Landauer formula. At a low temperature, the I-V curve is generally given by:

$$\bar{I} = \frac{e}{h}\int_{\mu_r}^{\mu_l} \mathrm{Tr}[\overline{\Gamma_l G^{\mathcal{R}}\Gamma_r G^{\mathcal{A}}}]dE. \tag{3}$$

The integrand of the above expression is the transmission coefficient where the impurity average, once again, correlates the retarded $G^{\mathcal{R}}$ and advanced $G^{\mathcal{A}}$ Green's functions. Evaluation of this correlation also involves a vertex correction, in this case with respect to one of the $\Gamma_{l,r}$, and is unavoidable even for the equilibrium situations [8,15]. The averaged transmission coefficient $\bar{T}(E)$ is calculated by Eq. (31) in the supplemental material [14].

As an important application of the NEGF-DFT-NVC formalism, we have investigated a disordered MTJ shown in Fig. 1, which consists of a vacuum (Vac) tunnel barrier sandwiched by two Fe leads. The Fe/Vac interface has roughness disorder, which substantially influences spin-dependent transport at equilibrium [16]. Here we focus on nonequilibrium. In our Fe/Vac/Fe MTJ, the interface roughness is present in one atomic layer on both left or right Fe/Vac interfaces with x and $1-x$ Fe atoms, respectively, and vacuum on the rest of the sites. The scattering region consists of ten perfect atomic layers of Fe oriented along (100) on the left and right ending with the rough interface sandwiching four vacuum layers. The scattering region is connected to perfect Fe left or right leads extending to $z = \pm\infty$. Because the entire structure, after impurity average, is periodic along the transverse x and y directions, we found that very careful two-dimensional BZ sampling is necessary in calculating the density matrix: We use 200×200 k mesh to ensure excellent numerical convergence. For the I-V curve calculation [Eq. (3)], 300×300 BZ k mesh is used for each point in the energy integration. For other DFT details, we follow standard TB-LMTO literature [16].

Figure 2(a) is a semilog plot of equilibrium ($V_b = 0$) conductance versus disorder x for both spin-up and -down channels $G_\uparrow$ and $G_\downarrow$, respectively. The four curves correspond to magnetic moments of the two Fe leads having parallel or antiparallel configurations (PC or APC). Since the left interface is chosen to be Fe_xVac_{1-x} while the right is $Fe_{1-x}Vac_x$, $G_{\uparrow,\downarrow}$ are both symmetric about $x = 0.5$ in PC (black squares and red circles, respectively). For APC, they are not symmetric but satisfy $G_\uparrow(x) = G_\downarrow(1-x)$, as expected. Impurity scattering changes all spin-dependent conductances; the most dramatic change is seen in $G_\downarrow$ in PC [red circles in Fig. 2(a)]. It was well known [17] that, for perfect interfaces, the surface electronic states of Fe give resonance transmission. These resonances are destroyed rapidly by the interface disorder as x changes from zero to 50% leading to the drastic reduction of $G_\downarrow$ in PC. An important device merit for MTJ is the tunnel magnetoresistance ratio (TMR) defined by total tunneling currents for PC and APC: $\mathrm{TMR} = (I^{\mathrm{PC}} - I^{\mathrm{APC}})/I^{\mathrm{APC}}$. At equilibrium when all currents vanish, we use equilibrium conductances to calculate the TMR. Figure 2(b) plots the equilibrium TMR versus x showing a dramatic effect of disorder. In particular, the TMR drops to very small values, even to slightly negative values, as x is increased from zero. These equilibrium features are consistent with previous supercell calculations [16].

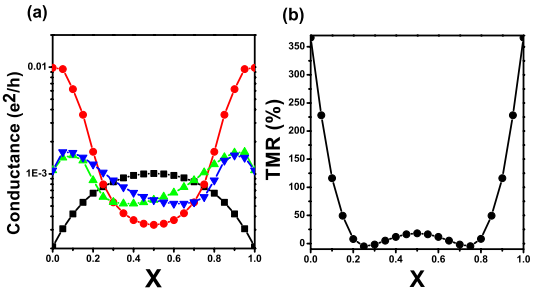

FIG. 2 (color online). (a) Conductance $G_{\uparrow,\downarrow}$ versus disorder x at equilibrium. Red circles: $G_\downarrow$ in PC; black squares: $G_\uparrow$ in PC. Blue down-triangles: $G_\downarrow$ in APC; green up-triangles: $G_\uparrow$ in APC. (b) The TMR versus x.

We now investigate nonequilibrium properties when $V_b \neq 0$ so that current flows through. To show the importance of NVC, we have calculated I-V curves at $x = 0.05$ by including the vertex correction only at the level of transmission coefficient, i.e., without NVC in the NEGF-DFT self-consistent iterations of the density matrix: The solid (green) lines in Fig. 3(a) plot this result. In comparison, the dashed (red) lines plot the full results where NVC is included. The substantial differences indicate that NVC is extremely important for obtaining correct results at nonequilibrium. Furthermore, if the vertex correction is neglected at the transmission calculation level, i.e., neglecting the second term of Eq. (31) of the supplemental material [14], the full NVC results (dashed lines) change to open circles and open squares in Fig. 3(a), again showing the importance of vertex correction. Figure 3(b) and its inset plot the TMR versus bias for four values of $x = 0.0$, 0.05, 0.3, and 0.5, obtained by the full NVC formalism. For zero or small values of x, the TMR reduces with V_b as is often seen in experimental measurements [18]. For larger x, for instance, $x \sim 0.5$, the TMR can go negative as V_b is increased. Indeed, experimental measurements had seen [19] a negative TMR at large V_b, although for different MTJs and possibly a different physical origin. Very dramatically, at $x = 0.3$, the entire TMR curve is negative:

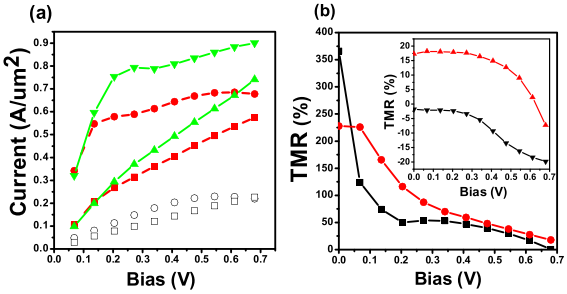

FIG. 3 (color online). (a) Comparison of I-V curves with disorder $x = 0.05$. Solid lines (green): Current for PC (down-triangles) and APC (up-triangles) without using NVC in a density matrix self-consistent iteration. Dashed (red) lines: Current for PC (solid circles) and APC (solid squares) using the full NVC theory. Open circles (PC) and open squares (APC) are full NVC data but neglecting vertex correction in the transmission calculation. (b) The TMR versus bias voltage V_b for four different values of x. The main figure is for $x = 0.0$ (black squares) and $x = 0.05$ (red circles); the inset is for $x = 0.3$ (black down-triangles) and $x = 0.5$ (red up-triangles).

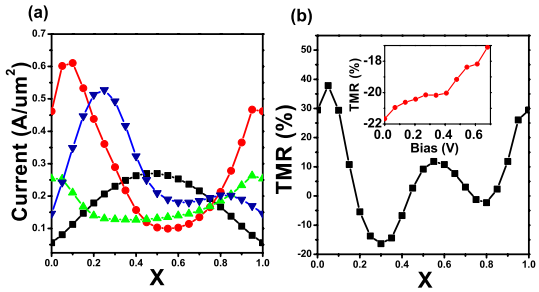

FIG. 4 (color online). (a) Spin-polarized currents versus disorder x at bias $V_b = 0.544$ V for PC and APC. Red circles and black squares: Spin-polarized currents for spin-up and -down in PC; green up-triangles and blue down-triangles: spin-polarized currents for spin-up and -down in APC. (b) The TMR versus x at the same V_b. Inset in (b): The TMR versus V_b for a device where the left and right interfaces have different values of x—on the left interface, $x = 0.3$; on the right, $x = 0.05$.

Here the absolute value of the TMR actually increases with V_b (see inset). These behaviors of the TMR strongly suggest that interface disorder plays very important roles for nonequilibrium spin injection.

Figure 4 plots spin-polarized currents and the TMR versus disorder x at $V_b = 0.544$ V. This is to be compared with Fig. 2, where $V_b = 0$. A finite bias breaks the left-right symmetry of the atomic structure, and, therefore, the spin-polarized currents do not have a symmetric behavior about $x = 0.5$ anymore. Both spin-polarized currents [Fig. 4(a)] and the TMR [Fig. 4(b)] vary with disorder x in substantial ways. In particular, the TMR rapidly dips to negative values when x is increased to about 20%. So far, we have focused on devices where the left has a $\mathrm{Fe}_x\mathrm{Vac}_{1-x}$ interface while the right has $\mathrm{Fe}_{1-x}\mathrm{Vac}_x$. We have also applied the NEGF-DFT-NVC formalism to devices where the left and right interfaces are disordered totally differently. The inset in Fig. 4(b) plots the TMR for such a system where the left interface has $x = 0.3$ while the right interface has $x = 0.05$. For this system, the TMR is negative, and its absolute value decreases as V_b is increased, which is qualitatively similar to what was discussed above.

In summary, we have developed a nonequilibrium vertex correction theory and its associated software for analyzing quantum transport properties of disordered nanoelectronic devices at nonequilibrium. The impurity averaging of the nonequilibrium density matrix is facilitated by the NVC that is related to quantum statistical information of the device scattering region. Our NEGF-DFT-NVC theory has several desired features, including atomistic first principles, nonequilibrium, an efficient configurational average, and self-consistency. This allows us to analyze nonequilibrium quantum transport of realistic device structures including realistic atomic substitutional impurities. By using this tool, we have calculated nonlinear spin-polarized currents in Fe/Vac/Fe MTJ with interface roughness disorder and found that the effects of NVC can play a dominant role in determining the properties of spin injection.

We gratefully acknowledge useful discussions with Zhanyu Ning, Wei Ji, Dr. Lei Liu, and Dr. Eric Zhu. This work is supported by NSERC of Canada, FQRNT of Quebec, and CIFAR (H. G.). K. X. is supported by NSF-China (No. 10634070) and MOST (No. 2006CB933000 and No. 2006AA03Z402) of China. We are grateful to RQCHP for providing a computation facility.

[1] T. Markussen, R. Rurali, A. P. Jauho, and M. Brandbyge, Phys. Rev. Lett. **99**, 076803 (2007).
[2] A. M. Bratkovsky, Phys. Rev. B **56**, 2344 (1997); E. Y. Tsymbal, A. Sokolov, I. F. Sabirianov, and B. Doudin, Phys. Rev. Lett. **90**, 186602 (2003).
[3] H. Ohno, Science **281**, 951 (1998).
[4] W. Ren, Z. Qiao, J. Wang, Q. Sun, and H. Guo, Phys. Rev. Lett. **97**, 066603 (2006).
[5] P. Soven, Phys. Rev. **156**, 809 (1967); B. Velický, S. Kirkpatrick, and H. Ehrenreich, Phys. Rev. **175**, 747 (1968).
[6] W. M. Temmerman, B. L. Gyorffy and G. M. Stocks, J. Phys. F **8**, 2461 (1978); G. M. Stocks and H. Winter, Z. Phys. B **46**, 95 (1982); N. Stefanou, R. Zeller, and P. H. Dederichs, Solid State Commun. **62**, 735 (1987).
[7] I. Turek *et al.*, *Electronic Structure of the Disordered Alloys, Surfaces and Interfaces* (Kluwer, Boston, 1997); J. Kudrnovský and V. Drchal, Phys. Rev. B **41**, 7515 (1990); J. Kudrnovský, V. Drchal, and J. Masek, Phys. Rev. B **35**, 2487 (1987).
[8] K. Carva, I. Turek, J. Kudrnovský, and O. Bengone, Phys. Rev. B **73**, 144421 (2006).
[9] J. Taylor, H. Guo, and J. Wang, Phys. Rev. B **63**, 121104(R) (2001); **63**, 245407 (2001); D. Waldron, P. Haney, B. Larade, A. MacDonald, and H. Guo, Phys. Rev. Lett. **96**, 166804 (2006).
[10] S. Datta, *Electronic Transport in Mesoscopic System* (Cambridge University Press, Cambridge, England, 1995).
[11] G. D. Mahan, *Many-Particle Physics* (Plenum, New York, 1981).
[12] O. K. Andersen and O. Jepsen, Phys. Rev. Lett. **53**, 2571 (1984).
[13] S. V. Faleev, F. Leonard, D. A. Stewart, and M. vanSchilfgaarde, Phys. Rev. B **71**, 195422 (2005).
[14] See EPAPS Document No. E-PRLTAO-100-020817 for supplemental material. For more information on EPAPS, see http://www.aip.org/pubservs/epaps.html.
[15] B. Velický, Phys. Rev. **184**, 614 (1969).
[16] P. X. Xu *et al.*, Phys. Rev. B **73**, 180402(R) (2006).
[17] J. A. Stroscio, D. T. Pierce, A. Davies, R. J. Celotta, and M. Weinert, Phys. Rev. Lett. **75**, 2960 (1995); O. Wunnicke *et al.*, Phys. Rev. B **65**, 064425 (2002).
[18] R. Jansena and J. S. Moodera, Appl. Phys. Lett. **75**, 400 (1999); S. S. P. Parkin *et al.*, Nat. Mater. **3**, 862 (2004); S. Yuasa *et al.*, Nat. Mater. **3**, 868 (2004).
[19] J. S. Moodera *et al.*, Phys. Rev. Lett. **83**, 3029 (1999).